Assessing the Pitting Corrosion Resistance of Oilfield Nickel Alloys at Elevated Temperatures by Electrochemical Methods

Helmuth Sarmiento Klapper[‡,*] *and Raul B. Rebak*[**]

ABSTRACT

Nickel alloys are broadly used in upstream oil and gas applications as a result of an advantageous set of properties including high mechanical strength accompanied by good ductility and toughness, excellent localized and environmentally assisted cracking resistance, and remarkable thermal stability. In general, their pitting corrosion resistance is ranked by calculating their pitting resistance equivalent (PRE) based on alloying element content, or by measuring the critical pitting temperature (CPT) in immersion tests in concentrated oxidizing acidic electrolytes. In spite of the fact that both concepts are crosslinked, the determination of CPTs is, from both approaches, clearly the best way to infer pitting corrosion resistance in service. Nevertheless, many of the electrolytes typically used for assessing CPTs suffer decomposition at temperatures higher than 85°C. Therefore, highly alloyed nickel alloys having CPT higher than 85°C cannot be ranked in these electrolytes. Electrochemical methods used to assess the pitting and repassivation potentials, which are well known for characterizing the pitting susceptibility of metallic alloys, emerge as one option to rank these at high temperatures. In the current study, the pitting corrosion resistance of four precipitation hardenable nickel alloys was electrochemically determined in 80,000 mg/L chloride solutions at ambient temperature, 80°C, and 150°C. Experimental results have shown that electrochemical methods such as open-circuit potential measurements and cyclic potentiodynamic polarization tests are suitable for ranking highly alloyed nickel alloys in chloride-containing environments at high temperatures. In addition, it was confirmed that the pitting corrosion resistance of these alloys was strongly influenced by its molybdenum content.

KEY WORDS: cyclic potentiodynamic polarization, nickel alloys, oil and gas, pitting corrosion, pitting susceptibility factor

INTRODUCTION

Corrosion-resistant alloys (CRAs) for upstream oil and gas applications are defined as alloys that are resistance to corrosion in applications where carbon and low alloyed steel suffer corrosion.[1] CRAs included a large number of alloys from 13% chromium containing stainless steel to highly alloyed iron-, nickel-, and cobalt-based alloys. Nickel (Ni) alloys, especially those strengthened by precipitation-hardening (PH) or by cold-working, are widely used in oilfield upstream technology, preferentially in hot downhole environments that involve corrosive gases such as CO_2 and H_2S.[1] Two Ni alloys favored by the oil and gas industry are alloys UNS N06625[(1)] and UNS N07718. However, UNS N07718 is often preferred due to its higher mechanical strength. One of the large advantages of Ni alloys over stainless steels is their resistance to stress corrosion cracking (SCC), which chronically plagues the performance of stainless steels in every industrial application.[2] Ni alloys, however, are not immune to localized corrosion and environmentally assisted cracking in upstream oilfield environments.[3-6]

Submitted for publication: June 7, 2016. Revised and accepted: March 20, 2017. Preprint available online: March 20, 2017, http://dx.doi.org/10.5006/2161.

‡ Corresponding author. E-mail: helmuth.sarmiento-klapper@bakerhughes.com.

* Baker Hughes, Center for Materials Research, Baker-Hughes-Strasse 1, D-29221 Celle, Germany.

** GE Global Research, 1031 Ardsley Rd, Schenectady, NY 12308.

(1) UNS numbers are listed in *Metals and Alloys in the Unified Numbering System*, published by the Society of Automotive Engineers (SAE International) and cosponsored by ASTM International.

ISSN 0010-9312 (print), 1938-159X (online)
17/000109/$5.00+$0.50/0

The pitting resistance equivalent (PRE) is commonly used to rate the pitting corrosion resistance of stainless steels and Ni alloys. ISO 21457,[7] for instance, includes recommendations for materials selection based on PRE. It is a relationship of the mass fraction of the elements chromium (Cr), molybdenum (Mo), tungsten (W), and nitrogen (N) in the alloy. The PRE concept derives from the pitting corrosion work done by Lorentz and Medawar on stainless steels.[8] Renner extended the use of statistical correlations between the chemical composition of stainless steels and their critical pitting temperature (CPT) to Ni alloys.[9] Consequently, both concepts, PRE and CPT, are related to some extent. Even though the use of the PRE to rank alloys is highly resisted in the scientific community, there is general consensus that alloys having high PRE own superior resistance to localized corrosion. It could not be different as Cr controls passive film formation and breakdown potential,[10] while Mo contributes the most to the repassivation ability of the alloy regardless its matrix (iron, nickel, cobalt) after pit initiation.[10-11] Tungsten is also considered in the majority of the equations used to calculate PRE and its effect on localized corrosion resistance of passive alloys is apparently similar to that from Mo.[11] As a result of the fact that the solubility of N in Ni alloys is much lower than in stainless steels, N is seldom purposely added in these alloys. Several empirical relationships include different factors for quantifying the effect of Mo, N, and W, and some others, especially for Ni alloys, including niobium (Nb) and tantalum (Ta) have been suggested.[12-14] There are more equations for calculating the PRE than experimental results that support a particular empirical correlation but all of them are essentially the same. Table 1 includes the nominal compositions[15] and the corresponding PRE values of several Ni alloys typically used in oilfield applications. The PRE was calculated using the values in mass percent listed in Table 1, and the equation specified in the ANSI/NACE MR0175/ISO 15156 standard.[16] In general, CRAs used in oilfield technology are classified in alloys with PRE ≥ 40 and those with PRE < 40, where the former are considered as highly resistant to localized corrosion and can, therefore, be used in aerated seawater without cathodic protection (CP).[7,16] Alloys having a PRE less than 40, including the first four Ni alloys listed in Table 1, are not recommended for seawater service without CP because of the danger of localized corrosion, especially crevice corrosion, at open-circuit potential (OCP) conditions.[7]

TABLE 1

Critical Pitting Temperatures of Oilfield Ni Alloys in Different Testing Environments

	Element (wt%)				CPT (°C)			
UNS	Cr	Mo	W	PRE	Env1[(A)]	Env2[(B)]	Env3[(C)]	Env4[(D)]
N07718	19.0	3.0		29	45	45		
N08825	21.5	3.0		31	30		25	
N09925	21.0	3.0		31	35			
N09946	21.5	3.5		33	45			
N07716	21.0	8.0		47	>85			
N07725	21.0	8.0		47	>85	75		
N06625	21.5	9.0		51	>85	75	90	41
N06022	22.0	13.0	3.0	65	>85	120	150	
N10276	16.0	16.0	4.0	75	>85	105	150	83
N06059	23.0	16.0		76	>85	>120		100
N07022	21.0	17.0	1.0	79	>85	>120		
N06686	21.0	16.0	3.7	80	>85	>120		

(A) According to ASTM G48 Method C in 6% $FeCl_3$ + 1% HCl.[9]
(B) 11.5% H_2SO_4 + 1.2% HCl + 1% $FeCl_3$ + 1% $CuCl_2$.
(C) 4% NaCl + 0.1% $Fe2(SO_4)_3$ + 0.01 M HCl.
(D) 4.5 M $CaCl_2$.[10]

The critical pitting and crevice temperatures, in contrast to PRE, are determined experimentally. These are the minimum temperatures to initiate pitting and crevice attack in passive alloys and are frequently used to rate the resistance to localized corrosion of Ni alloys used in oilfield technology. According to Newman, the CPT defines a propagation-related transition below which metastable pits will not grow stably.[17] ASTM G48[18] Method C describes immersion tests in acidified ferric chloride solution for determining the CPT of Ni alloys. Nevertheless, other environments such as the so-called "green death" solution,[19] consisting of 11.5% H_2SO_4 + 1.2% HCl + 1% $FeCl_3$ + 1% $CuCl_2$ and concentrated brines,[20] have been used. Table 1 includes CPT values for several Ni alloys used in oilfield technology in different test environments (Env) mainly reported by primary metal producers of Ni alloys.

One significant drawback of the test solutions typically used for determining the CPT is, however, their limited thermal stability at elevated temperatures. For example, the maximum test temperature in the ferric chloride solution according to ASTM G48 is 85°C.[18] In addition, the green death solution becomes chemically unstable above 120°C. Therefore, results that reports CPT values beyond 120°C in this environment are questionable.[14,20] On the other hand, as shown in Table 1, highly alloyed Ni-Cr-Mo alloys may not exhibit pitting corrosion at temperatures below 120°C and cannot be ranked using these environments. Upstream oilfield environments often involve temperatures beyond 120°C, though. Therefore, electrochemical techniques in thermally stable electrolytes are preferred for benchmarking Ni alloys regarding their pitting corrosion resistance at high temperatures (T > 120°C). While the majority of the characterization of Ni alloys has been concentrated on its performance in deaerated H_2S/CO_2-bearing environments at high temperatures, surprisingly very little attention has been paid on the pitting corrosion susceptibility of these alloys in halide bearing solutions at high temperatures, which are also very relevant to oil and gas upstream operations. In this study electrochemical techniques have been used for benchmarking the pitting corrosion resistance of some Ni alloys

commonly used in oilfield technology. The obtained experimental results are discussed using Galvele's pit growth model included in his original publication entitled "Transport Processes and the Mechanism of Pitting of Metals."[21] In this regard, 2016 marked the 40th anniversary of the publication of Prof. Galvele's work in the *Journal of the Electrochemical Society*, which is among the 100 most cited papers in the history of that journal.

EXPERIMENTAL PROCEDURES

Materials and Test Setup

The pitting corrosion resistance of the Ni alloys listed in Table 2 have been determined by electrochemical methods. The actual chemical composition of the investigated materials is included in Table 2. Alloys 718 (UNS N07718), 945X[†] (UNS N09946), and 716 (UNS N07716) were tested in the age-hardened condition according to the heat treatments described in API 6ACRA,[22] leading to a minimum yield strength of 965 MPa. Alloy C-22HS[†] (UNS N07022) was tested in the cold-worked condition. Experiments were conducted at ambient temperature (22±2°C) and 80±2°C, at atmospheric pressure, and at 150±5°C (ca. 500 kPa). For the electrochemical measurements at room temperature (RT) and at 80°C, a conventional three-electrode configuration including a KCl-saturated Ag/AgCl reference electrode (200 mV_{SHE}) and one TiO-covered Ti counter electrode was used. Measurements at 150°C were performed in a fully controlled autoclave using a KCl-saturated Ag/AgCl reference electrode suitable for high-temperature applications. Each experimental condition was evaluated three times in separate experiments to assess the reproducibility of the results. For each test a new specimen and fresh prepared test solution were used. L-shaped specimens with a measuring surface of ca. 845 mm^2 were cut by wire electrical discharge machining (EDM) from bars in longitudinal direction. Prior to the electrochemical tests the surface of the samples was treated by mechanical grinding consecutively with SiC emery papers up to 360 grit prior to each experiment. Test environments have been deaerated in near-neutral (pH 6.7 at 22°C) NaCl solutions having 80,000 mg/L Cl^-. The fresh prepared test solution was then purged 30 min with nitrogen before the electrochemical test was started.

Electrochemical Methods

The OCP was monitored for 60 min before the cyclic potentiodynamic polarization test was conducted. For measurements at 150°C the polarization scan was started after 120 min as the first 60 min were necessary to reach the target test temperature in the autoclave. In contrast, the electrochemical tests at RT and at 80°C were started immediately after surface preparation because the test solution was tempered in advance.

[†] Trade name.

TABLE 2
Chemical Composition of the Investigated Ni Alloys (wt%)

Alloy	UNS	C	Cr	Mo	Ni
718	N07718	0.020	18.6	3.0	54.5
945X	N09946	0.010	20.6	3.2	53.5
716	N07716	0.013	20.9	8.1	61.0
C-22HS	N07022	0.002	20.2	16.4	Balance
Alloy	**UNS**	**Al**	**Nb**	**Ti**	**W**
718	N07718	0.45	5.03[(A)]	0.83	–
945X	N09946	0.11	4.07	1.53	–
716	N07716	0.23	3.70[(A)]	1.42	–
C-22HS	N07022	0.27	–	–	0.03

[(A)] Nb + Ta.

The potential scan was started at 100 mV below the OCP with a scan rate of 0.2 mV/s. The pitting potential (E_{pit}) was defined as the potential at which the current density reached 100 μA/cm^2. At this point the direction of the polarization scan was switched in the cathodic direction to assess the repassivation potential of the material (E_{rp}). The repassivation potential has been defined as the potential at which the current density returned to 100 μA/cm^2 during the reverse scan.

RESULTS

Electrochemical results have confirmed the excellent pitting corrosion resistance of all of the investigated Ni alloys at room temperature. As shown in Figure 1, a stable passive state characterized by very low corrosion current densities, typically lower than 10^{-6} A/cm^2, was measured over a broad range of polarization potentials regardless of the chemical composition of the alloys. In addition, passivity breakdown potentials were more noble than 1.1 V_{SHE} and excellent repassivation ability characterized by small hysteresis was determined in all cases. No pits were detected during microscopic inspection of the specimens after potentiodynamic polarization tests at RT. Therefore, the

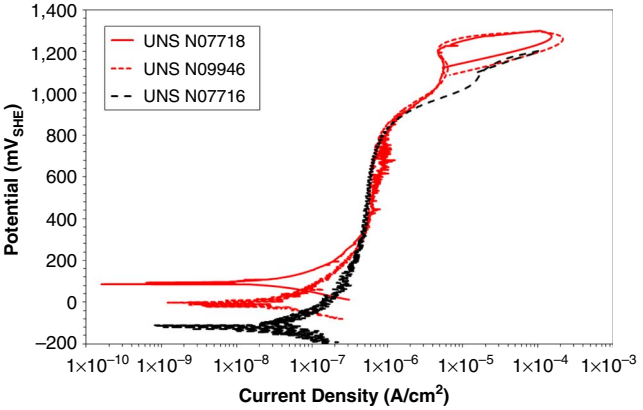

FIGURE 1. *Typical cyclic potentiodynamic polarization curves of several Ni alloys in 80,000 mg/L Cl-containing solution of near-neutral pH at 22°C.*

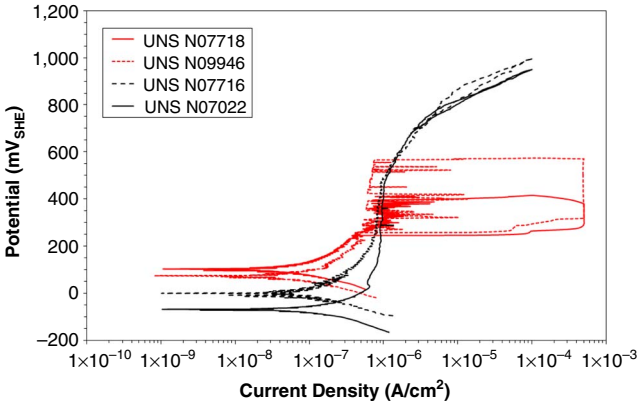

FIGURE 2. *Typical cyclic potentiodynamic polarization curves of several Ni alloys in 80,000 mg/L Cl-containing solution of near-neutral pH at 80°C.*

observed increase in the current density at high polarization potentials can be attributed to early stages of transpassive dissolution of the Ni alloys rather than to pitting. With increasing the test temperature to 80°C, the pitting corrosion susceptibility of UNS N07718 and UNS N09946 was significantly increased. Figure 2 shows typical cyclic potentiodynamic polarization curves obtained in the 80,000 mg/L Cl-containing solution at 80°C for all of the investigated alloys. The average pitting corrosion potential (E_{pit}) of UNS N07718 and UNS N09946 was 416±10 mV_{SHE} and 559±21 mV_{SHE}, respectively. The repassivation potentials (E_{rp}) were, in contrast to the pitting potential, very similar being 260±4 mV_{SHE} for UNS N07718, and 303±21 mV_{SHE} for UNS N09946. Metastable pitting occurred at polarization potentials more noble than 250 mV_{SHE} on both alloys. The E_{pit} values measured on both alloys at 80°C were 300 mV higher compared to the corresponding corrosion potential (E_{corr}), and the E_{rp} values were in all cases more positive to the OCP. On the other hand, the high Mo-containing UNS N07716 and UNS N07022 were not prone to pitting corrosion and showed transpassive dissolution instead of pitting at very high polarization

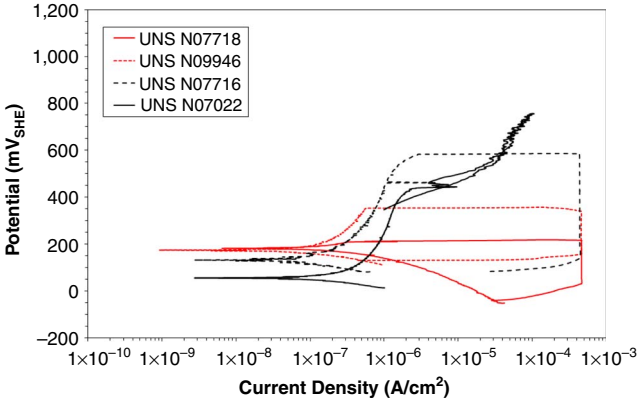

FIGURE 3. *Typical cyclic potentiodynamic polarization curves of several Ni alloys in 80,000 mg/L Cl-containing solution of near-neutral pH at 150°C.*

potentials. At 150°C UNS N07716 became susceptible to pitting at polarization potentials around 600 mV_{SHE} and repassivated at potentials a few millivolts more positive than its E_{corr}. In contrast, the E_{rp} values for UNS N07718 and UNS N09946 were always lower than their corresponding corrosion potentials and, as shown in Figure 3, their pitting potentials were a few hundreds of millivolts more positive compared to E_{corr}. In contrast, no pitting was observed on UNS N07022 but the passivity breakdown potential was reduced about 200 mV compared to the potential determined at 80°C.

DISCUSSION

Electrochemical results have shown that elevated temperatures affected significantly the pitting corrosion susceptibility of the investigated Ni alloys. To quantify the pitting corrosion resistance of the materials, the pitting susceptibility factor (PSF) was calculated according to Equation (1) using the electrochemical parameters obtained from the cyclic potentiodynamic polarization curves and the OCP measurements. The PSF was introduced in the past for quantifying the pitting susceptibility of stainless steels,[23] and is the quotient of the repassivation ability of the material represented by the difference between the pitting and the repassivation potentials, and the resistance of the material to pit initiation represented by the difference between their pitting and the OCPs. The OCP value measured after 1 h of exposure at the test temperature was used in Equation (1) for calculating the PSF. But, it could be replaced by E_{corr} determined from the potentiodynamic polarization curve, as a good correlation between both values should be observed:

$$PSF = \frac{E_{pit} - E_{rp}}{E_{pit} - OCP} \quad (1)$$

Equation (1) led to a mathematical fallacy when pitting corrosion occurs at OCP conditions, and, in consequence, the E_{pit} determined electrochemically becomes identical to the OCP. This is typically accompanied by an increase in the corrosion current density. Therefore, PSF values can be used to quantify pitting corrosion susceptibility as long as the tested material remains passive and exhibits a repassivation potential during the polarization scan in cathodic direction. Typical PSF values of passive alloys rank between 0 ($E_{pit} = E_{rp}$) and 5. Values equal or larger than 1 indicate susceptibility to pitting corrosion of the material. This threshold value for the PSF has been validated in the past for stainless steels in chloride-containing solutions.[23] PSF values greater than 1 are possible but no correlation between the magnitude (pit density and pit depth) of pitting damage and PSF values has been established yet. It is matter of current research work. This correlation is expected to be dependent upon the type of material and the testing environment.

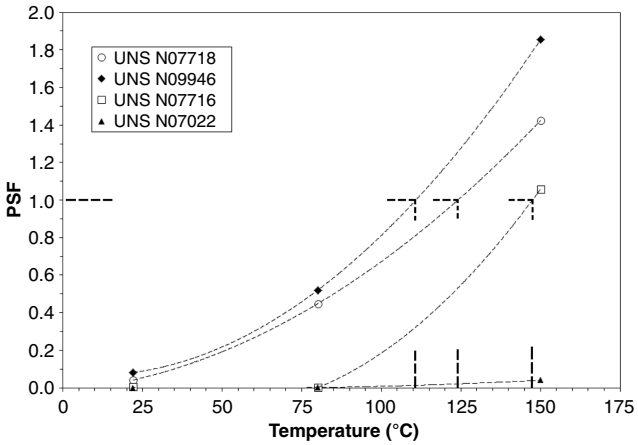

FIGURE 4. *Temperature dependence of PSF values of different Ni alloys obtained in deaerated near-neutral 80,000 mg/L Cl-containing solutions.*

Figure 4 shows the PSF values calculated using the average of the electrochemical parameters obtained for each of the investigated alloys in the deaerated Cl-containing solution as a function of the temperature. All of the investigated Ni alloys had very low PSF values at 22 ±2°C and are, therefore, not expected to be prone to pitting corrosion at ambient temperature. This agrees with results recently obtained on UNS N07718 in deaerated chloride-containing solutions.[24] As the temperature was increased, the pitting susceptibility of these alloys characterized by the PSF increased considerably. While 3 wt% Mo-containing alloys did exhibit pitting corrosion during the anodic polarization scan at 80°C, highly-Mo alloyed Ni alloys were not prone to pitting and showed only transpassive dissolution at very noble polarization potentials (Figure 2). None of the calculated PSF values for the Ni alloys at 80°C, however, exceeded the susceptibility threshold (Table 3). It suggests that the investigated Ni alloys are not susceptible to pitting corrosion in the test environment used in this study at 80°C. Based on the correlations included in Figure 4, the 3 wt% Mo-containing alloys would become prone to pitting corrosion first at temperatures beyond 100°C. In spite of the fact that both, the results from tests according to ASTM G48 Method C[18] and the experimental results obtained in this study did not show any significant difference in terms of pitting resistance between UNS N07718 and UNS N09946, the experimental results deviate from those reported in Table 1, which indicate that both UNS N07718 and UNS N09946 are susceptible to pitting corrosion at 45°C. This can be partially explained by the significant difference in pH between the acidified ferric chloride test solution specified in ASTM G48 Method C[18] and the near-neutral solution used in this study. It also points out the limited extrapolation capability of standardized CPT test results to real service conditions, like those observed in certain upstream oilfield applications, which can deviate from a concentrated oxidizing acidic electrolyte. The results obtained by the methodology described in ASTM G48 Method C[18] can, therefore, be used to benchmark the pitting resistance of Ni alloys at temperature up to 85°C rather than to infer materials performance for a particular application. The difference observed between the experimental results and those according to ASTM G48 Method C[18] also demonstrates the relevance of pH in pit initiation of Ni alloys. On UNS N07718 a higher pitting potential was observed in high chloride-containing environments at 150°C when the pH of the electrolyte was raised to 10.[24] The repassivation potential, in contrast, was less noble than the corresponding OCP regardless the alkalinity of the environment. This suggests that once pits nucleate, the bulk pH of the test solution has little or no influence on the repassivation potential value, and pit propagation is mainly driven by the repassivation ability of the material at the particular conditions within the pit as explained in Galvele's acidification model.[21]

TABLE 3
PSF Values of Ni Alloys in 80,000 mg/L Cl-Containing Solution at Different Temperatures

		PSF		
Alloy	**UNS**	**RT**	**80°C**	**150°C**
718	N07718	0.04	0.45	1.42
945X	N09946	0.08	0.52	1.85
716	N07716	<0.01	<0.01	1.06
C-22HS	N07022	<0.01	<0.01	0.04

With increasing further the temperature to 150°C, the 8 wt% Mo-containing Ni alloy UNS N07716 also became susceptible to pitting corrosion according to the calculated PSF values (Table 3). It has to be noted that the pitting potential of UNS N07718 and UNS N09946 at 150°C (Figure 3) was in the range of the polarization potentials where metastable pitting corrosion was observed on these materials at 80°C (Figure 2). This indicates that the pit nucleation mechanism of these alloys is similar at both temperatures but as far as pits nucleate, they could propagate stably as a result of the lack of repassivation that occurs at 150°C. In fact, pit propagation characterized by potential transients were identified in the OCP time records of UNS N07718 and UNS N09946 (Figure 5) once the temperature of the electrolyte achieved the target temperature of 150°C and the OCP was close to the E_{pit} observed in the cyclic potentiodynamic polarization curves (Figure 3). The susceptibility of UNS N07718 to pitting corrosion in chloride-containing solutions at elevated temperatures has been demonstrated in the past.[24] In contrast to both 3 wt% Mo-containing alloys, UNS N07716 did not show any potential transient during the OCP measurements. The E_{pit} of UNS N07716 measured at 150°C was indeed 400 mV higher compared to its E_{corr}. The high PSF value calculated for UNS N07716 (Table 3) can, therefore, only be explained by the small difference between the E_{rp}

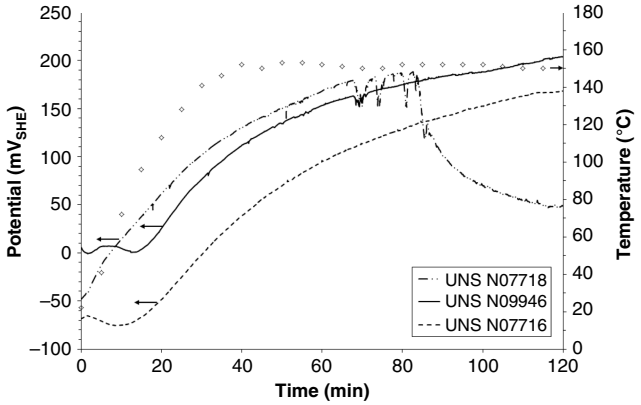

FIGURE 5. *OCP time records obtained on different Ni alloys in deaerated near-neutral 80,000 mg/L Cl-containing solutions.*

and the OCP measured on the material at 150°C in spite of the high Mo content in the material. Pits generated during the potentiodynamic polarization scan on UNS N07716 continued growing during the reverse scan due to the significant cathodic current delivered to the counter electrode by the potentiostat in order to keep the high anodic polarization potential. This is confirmed by the high current density, typically higher than 5×10^{-4} A/cm^2, measured before repassivation occurs. Metal cation salt hydrolysis supports acidification of the pit bottom previous to saturation and salt precipitation, as described in Galvele's model.[21] A similar behavior was observed for UNS N07718 and UNS N09946 at 80°C. Both alloys did not show pit propagation during the OCP measurements at 80°C even though metastable pitting was observed at polarization potentials slightly more positive compared to the measured OCP during the cyclic potentiodynamic tests (Figure 2). These observations suggest that the electrochemical parameters that characterize the pitting susceptibility of the material determined from cyclic potentiodynamic polarization scans should be treated carefully and always put into context by the electrochemical behavior of the material at OCP conditions (without polarization), as well as, if available, by results from long-term exposure tests.[25] These electrochemical parameters including the derived PSF values are relative rather than absolute values as a result of the fact that they are produced in an accelerated test and are influenced by the used testing parameters such as scan rate, exposed surface area as well as the selected current density threshold for the reverse scan. Additionally, these parameters describe the pitting susceptibility of the material only at the test conditions (electrolyte, temperature, surface condition), and cannot be extrapolated to other environmental conditions without further testing. On the other hand, electrochemical methods such as those used in the present study enable benchmarking Ni alloys in simulated environments, close to those expected in service, and at temperatures beyond the limits for the chemical stability of standardized and non-standardized test solutions for determining CPT values. PSF vs. temperature curves such as those included in Figure 4 can be used as reference for determining threshold temperatures in a particular environment. On the other hand, the lack of repassivation during the reverse scan under potentiodynamic control could also be used as an indication for susceptibility to crevice corrosion of the material as suggested by other authors.[26-27] In addition, models have been generated and validated by Anderko, et al., for predicting the localized corrosion resistance of CRAs including Ni alloys in oilfield environments using the difference between predicted OCP and E_{rp} values.[28-29]

A linear correlation was obtained between the Mo content in the evaluated Ni alloys and their pitting corrosion susceptibility described by the PSF at elevated temperatures. As expected, the obtained correlations have negative slope. It has been also seen that while the intercept increased considerably with increasing the temperature from 80°C to 150°C, the slope remained almost constant (Figure 6). Galvele, et al., studied the pitting corrosion behavior of 18 wt% Cr ferritic stainless steels containing different amounts of Mo from 0 wt% to 5 wt%.[30] It was found that increasing the amount of Mo in the alloy increased its pitting potential. They understood that Mo mainly changed the rate of pit propagation or reduced the kinetics of alloy dissolution inside the pit. According to Galvele,[21] the pitting potential of a given alloy in a neutral solution can be calculated by:

$$E_p = E_c^* + \eta + \Phi + E_{inh} \quad (2)$$

where E_p and E_c^* correspond to the pitting and corrosion potentials, respectively; η is the anodic polarization required to reach the critical current i_{crit} at the bottom of a pit; Φ is the ohmic potential drop along the pit; and E_{inh} is an additional polarization required in presence of buffers or inhibitors. Galvele and coworkers rationalized their findings by assuming that Mo changed

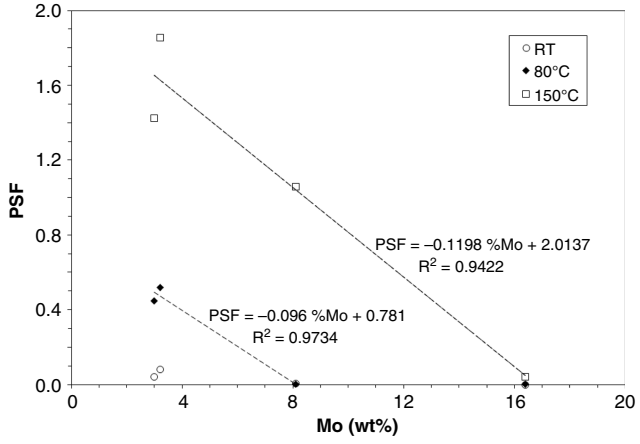

FIGURE 6. *Effect of Mo content in Ni alloys on the PSF values obtained in 80,000 mg/L Cl-containing solution at different temperatures.*

either η by reducing the dissolution rate of $CrCl_3$, or increased the E_c^* of the alloy in the localized acidified pit electrolyte. It is now understood that Mo may have little effect on pit initiation but is highly effective in accelerating the repassivation process of the alloy once pitting has initiated.[31] Considering that the investigated Ni alloys have similar Cr content (Table 2), the correlations shown in Figure 6 confirm that the pitting susceptibility of these alloys at elevated temperatures was mainly driven by their repassivation behavior, i.e., by their Mo content. Gruss, et al.,[32] compared the repassivation potentials of the Ni alloys 825 (UNS N08825), 625 (UNS N06625), and 22 (UNS N06022) using a similar methodology to that used in the present study but at lower temperatures. They reported an increase in the repassivation potential following the order: UNS N08825<UNS N06625<UNS N06022. As the amount of Cr in these alloys is similar (Table 1), the improved repassivation ability of UNS N06022 was explained in terms of its higher Mo content. Similar conclusions were drawn by Hayes, et al.,[10] Zadorozne, et al.,[33] and Hornus, et al.,[34] who observed during crevice corrosion tests that the repassivation potential of Ni-Cr-Mo alloys increased with the Mo content in the alloy. Electrochemical results obtained in this study suggest that pit initiation of Ni-Cr-Mo alloys in Cl-bearing environments is affected by the temperature necessary to maintain local dissolution of particular phases, most likely carbides, present in the austenitic matrix. The subsequent repassivation necessary to prevent pit propagation appears to be also controlled by the thermal stability of the insoluble molybdate protective layer. Mo and W deposition during crevice corrosion of NiCrMo alloys has been observed in the past by Shoesmith, et al.,[11,35] as well as by Shan and Payer.[36] However, the influence of temperature on these processes has received limited scientific attention and needs, therefore, confirmation by additional experimental work. On the other hand, only the highly Mo alloyed Ni alloy UNS N06022 has shown sufficient localized corrosion resistance at 150°C. Alloy 59 (UNS N06059), having a very similar Mo content to UNS N06022, has also shown outstanding pitting corrosion resistance in highly saline geothermal environments of near-neutral pH at 150°C.[37] By having high amounts of molybdenum in the alloy, the influence of temperature on pit nucleation and repassivation can be significantly reduced.

CONCLUSIONS

Based on the experimental results obtained in this study, the following conclusions can be drawn:

❖ Electrochemical methods such as open-circuit potential measurements and cyclic potentiodynamic polarization tests are suitable for ranking highly alloyed Ni alloys in chloride-containing environments at high temperatures where the determination of CPT values becomes problematic as a result of the limited thermal stability of the test solutions. Electrochemical results obtained in simulated environments close to real service conditions are also more meaningful for predicting Ni alloys' performance in terms of pitting corrosion resistance during operation when compared to assessments purely based on PRE or CPT values obtained in standardized solutions.

❖ The pitting susceptibility factor (PSF) that is calculated based on parameters obtained from cyclic potentiodynamic polarization tests was successfully used to quantify the pitting susceptibility of Ni alloys.

❖ The pitting corrosion resistance of four Ni alloys typically used in oilfield technology was electrochemically determined in 80,000 mg/L chloride solutions at temperatures up to 150°C. It was confirmed that the pitting corrosion resistance of these alloys at elevated and high temperatures is strongly influenced by its molybdenum content. While the 3% Mo-containing alloys were prone to pitting at temperatures around 120°C, only the highly Mo alloyed alloys have shown sufficient pitting corrosion resistance at temperatures beyond 120°C, which are encountered in some upstream oilfield applications.

ACKNOWLEDGMENTS

The authors would like to express their deepest gratitude to Prof. José Rodolfo Galvele for being a passionate advisor and mentor. His perennial footprint in corrosion science and engineering is an inspiring example for past, present, and future generations of corrosionists around the globe and especially in Latin America.

REFERENCES

1. P.R. Rhodes, L.A. Skogsberg, R.N. Tuttle, *Corrosion* 63 (2007): p. 63.
2. M. Speidel, *Metall. Trans.* 12 (1981): p. 779.
3. S. Huizinga, B. McLoughlin, W.E. Like, J.G. de Jong, "Offshore Nickel Alloy Tubing Hanger and Duplex Stainless Steel Piping Failure Investigations," CORROSION 2003, paper no. 129 (Houston, TX: NACE International, 2003).
4. T. Cassagne, M. Bonis, D. Hillis, C. Duret, "Understanding Field Failure of Alloy 718 Forging Materials in HP/HT Wells," EuroCorr 2008 (Edinburgh, United Kingdom: EFC, 2008).
5. S.S. Shademan, J.W. Martin, A.P. Davis, "UNS N07725 Nickel Alloy Connection Failure," CORROSION 2012, paper no. 01095 (Houston, TX: NACE, 2012).
6. P. Nice, R. Strong, W. Bailey, G. Rorvik, J.H. Olsen, T.G. Mobberley, "Hydrogen Embrittlement Failure of a Precipitation Hardened Nickel Alloy Subsurface Safety Valve Component Installed in a North Sea Seawater Injection Well," CORROSION 2014, paper no. 03992 (Houston, TX: NACE, 2014).
7. ISO 21457 Petroleum, "Petrochemical and Natural Gas Industries - Materials Selection and Corrosion Control for Oil and Gas Production Systems" (Geneva, Switzerland: ISO, 2010).
8. K. Lorenz, G. Médawar, *Thyssen-Forschung* 1 (1969): p. 97.
9. M. Renner, U. Heubner, M.B. Rockel, E. Wallis, *Mater. Corros.* 37 (1986): p. 183.
10. J.R. Hayes, J.J. Gray, A.W. Szmodis, C.A. Orme, *Corrosion* 62 (2006): p. 491.
11. N. Ebrahimi, P. Jakupi, J.J. Nöel, D.W. Shoesmith, *Corrosion* 71 (2015): p. 1441.

12. D.C. Agarwal, W.R. Herda, *Mater. Corros.* 48 (1997): p. 542.
13. E. Hibner, S. Tassen, J.W. Skogsberg, "Effect of Alloy Nickel Content vs. PREN on the Selection of Austenitic Oil Country Tubular Goods for Sour Gas Service," CORROSION 1998, paper no. 106 (Houston, TX: NACE, 1998).
14. S. Schmigalla, A. Heyn, *Mater. Corros.* 64 (2013): p. 700.
15. P. Crook, *ASM Handbook*, Vol. 13B (Materials Park, OH: ASM International, 2005), p. 228.
16. ANSI/NACE MR0175/ISO 15156, "Petroleum, and Natural Gas Industries—Materials for Use in H_2S-Containing Environments in Oil, and Gas Production," Section 6.3 (New York, NY: ANSI/NACE/ISO, 2009).
17. G. Frankel, G. Thornton, S. Street, T. Rayment, D. Williams, A. Cook, A. Davenport, S. Gibbon, D. Engelberg, C. Ornek, A. Mol, P. Marcus, D. Shoesmith, C. Wren, K. Yliniemi, G. Williams, S. Lyon, R. Lindsay, T. Hughes, J. Lutzenkirchen, S.T. Cheng, J. Scully, S.F. Lee, R. Newman, C. Taylor, R. Springell, J. Mauzeroll, S. Virtanen, S. Heurtault, J. Sullivan, *Faraday Discuss.* 180 (2015): p. 381.
18. ASTM G48, "Standard Test Methods for Pitting, and Crevice Corrosion Resistance of Stainless Steels, and Related Alloys by Use of Ferric Chloride Solution" (West Conshohocken, PA: ASTM International, 2015).
19. P.E. Manning, J.-D. Schöbel, *Mater. Corros.* 37 (1986): p. 137.
20. G. Riedel, C. Voigt, H. Werner, *Mater. Corros.* 48 (1997): p. 518.
21. J.R. Galvele, *J. Electrochem. Soc.* 123 (1976): p. 464.
22. API 6ACRA, "Age Hardened Nickel-Based Alloys for Oil Gas Drilling and Production Equipment" (Washington, DC: API, 2015).
23. H. Sarmiento Klapper, J. Stevens, "Influence of Alloying Elements on the Pitting Corrosion Resistance of CrMn-Stainless Steels in Simulated Drilling Environments," CORROSION 2015, paper no. 5527 (Houston, TX: NACE, 2015).
24. H. Sarmiento Klapper, J. Stevens, *Corrosion* 70 (2014): p. 899.
25. N. Sridhar, C.S. Brossia, D.S. Dunn, A. Anderko, *Corrosion* 60 (2004): p. 915.
26. B.E. Wilde, E. Williams, *Electrochim. Acta* 16 (1971): p. 1971.
27. E.B. Haugan, M. Næss, C. Torres Rodriguez, R. Johnsen, M. Iannuzzi, *Corrosion* 73 (2017): p. 53.
28. A. Anderko, N. Sridhar, C. Brossia, "Prediction of Corrosion of Nickel-Base Alloys and Stainless Steels in Oxidizing Environments Using Thermodynamic and Electrochemical Models," CORROSION 2005, paper no. 5053 (Houston, TX: NACE, 2005).
29. A. Anderko, G.R. Engelhardt, F. Gui, L. Cao, N. Sridhar, "Localized Corrosion of Corrosion Resistant Alloys in Environments Containing Hydrogen Sulfide," CORROSION 2015, paper no. 5562 (Houston, TX: NACE, 2015).
30. J.R. Galvele, J.B. Lumsden, R.W. Staehle, *J. Electrochem. Soc.* 125 (1978): p. 1204.
31. Z. Szklarska-Smialowska, *Pitting and Crevice Corrosion* (Houston, TX: NACE, 2005).
32. K.A. Gruss, G.A. Cragnolino, D.S. Dunn, N. Sridhar, "Repassivation Potential for Localized Corrosion of Alloys 625 and C22 in Simulated Repository Environments," CORROSION 1998 (Houston, TX: NACE, 1998).
33. N.S. Zadorozne, C.M. Giordano, M.A. Rodríguez, R.M. Carranza, R.B. Rebak, *Electrochim. Acta* 76 (2012): p. 94.
34. E.C. Hornus, C.M. Giordano, M.A. Rodríguez, R.M. Carranza, R.B. Rebak, *J. Electrochem. Soc.* 162 (2015), p. C105.
35. P. Jakupi, F. Wang, J.J. Noel, D.W. Shoesmith, *Corros. Sci.* 52 (2011): p. 1670.
36. X. Shan, J.H. Payer, *J. Electrochem. Soc.* 156 (2009): p. C313.
37. H. Sarmiento Klapper, R. Bässler, K. Weidauer, D. Stuerzbecher, *Corrosion* 68 (2012): p. 16001-1.